Journal of Geomine (2026), 4(2), 131-142
DOI: 10.22077/jgm.2026.10898.1070

Support of squeezing rocks in underground coal mines, case study: slope no. 2 of Parvadeh no. 1 mine

Hossain Noferesti[1]*, Mohsen Alizadeh Sani[2]

Received: 2026 Jan. 26, Revised: 2026 Jul. 07, Accepted: 2026 Aug. 23, Published: 2026 Sept. 17

ABSTRACT

Tunnel squeezing is one of the major challenges in mechanized longwall coal mining and is primarily caused by stress redistribution following coal extraction. In main gate tunnels, the support system is subjected to significant loads during panel extraction and longwall advancement. The Tabas Parvadeh No. 1 Coal Mine, which uses a mechanized longwall mining method, has experienced severe squeezing problems in its main gate tunnels at depths greater than 400 m. In certain sections, the magnitude of deformation following coal extraction has exceeded the capacity of the existing support system, necessitating the evaluation of alternative support designs. In this study, the squeezing behavior of the main roadways of the Parvadeh No. 1 Mine is investigated using the Hoek analytical method in conjunction with finite element modeling. Based on the results obtained, the tunnel support system has been redesigned to effectively withstand the squeezing pressures encountered at the current mining depth. It was determined that using TH40 steel arches installed at a spacing of 0.5 meters is sufficient to endure the pressures exerted by the roof and sidewalls. However, it is essential to also reinforce the tunnel floor with an additional support system, such as a concrete slab.

KEYWORDS

Squeezing, floor heave, Hoek analytical method, FEM, Parvadeh mine

I. INTRODUCTION

The extraction of coal through underground mining techniques has long been a fundamental aspect of the global energy landscape. As coal mining operations expand, the structural integrity of the surrounding geological formations becomes increasingly critical. Squeezing in coal mining tunnels is a critical issue that affects the safety and operational efficiency of underground mining operations. This phenomenon, characterized by the deformation of surrounding rock due to increased stress from overburden, has been extensively studied in the context of rock mechanics and mining engineering.

Squeezing occurs when the stress on the rock surrounding a mine tunnel exceeds its strength, leading to plastic deformation. According to Jaeger and Cook (1979), this phenomenon is particularly pronounced in soft or weak rock formations, where the material can yield under stress. Barton et al. (1974) identified that factors such as rock type, geological structure, and the depth of mining significantly influence the likelihood of squeezing. The transition from elastic to plastic behavior in rock is often governed by the Mohr-Coulomb failure criterion, which highlights the importance of understanding the mechanical properties of the rock mass.

Several studies have identified key factors contributing to the squeezing phenomenon. Cheng et al. (2009) emphasized the role of high in-situ stress conditions, which can be exacerbated by mining activities. The orientation of the mine layout relative to natural geological stresses can also influence the degree of squeezing experienced. Additionally, Li et al. (2015) found that water infiltration can weaken rock materials, further increasing susceptibility to deformation. The implications of squeezing for coal mining operations are significant. Kang et al. (2016) noted that excessive squeezing can lead to tunnel collapse, posing severe safety risks for miners and resulting in costly downtime for operations. Moreover, Zhang et al. (2018) reported that frequent encounters with squeezing conditions necessitate increased support measures, such as rock bolts and shotcrete, which can inflate operational costs and reduce overall efficiency. To address the challenges posed by squeezing, researchers have proposed various mitigation strategies. Yuan et al.

[1] Department of Mining Engineering, Faculty of Engineering, University of Birjand, Birjand, Iran, [2] MEMRADCO, Parvadeh 3 Mine, Tabas, Iran
H. Noferesti: hnoferesty@birjand.ac.ir

(2020) suggested using pre-mining geological investigations to assess rock stability and inform design choices for tunnel support systems. Advanced monitoring techniques, including ground-penetrating radar and stress measurement devices, have also been recommended to provide real-time data on rock behavior during mining operations (Wang et al., 2021). Furthermore, numerical modeling has become an essential tool for predicting squeezing behavior and optimizing support strategies (Zhao et al., 2019). Huang et al. (2022) proposed a method for predicting tunnel squeezing using a combination model of Support Vector Machine (SVM) and Back Propagation (BP) neural networks. Their study emphasizes the advantages and positive outcomes of this model. However, it is also important to consider the potential disadvantages and limitations of integrating SVM and BP. Najm and Daraei (2023) explored the challenges of rock squeezing in the longest highway tunnel in the Middle East, identifying two primary failure mechanisms that could threaten structural integrity. Furthermore, Luo et al. (2024) developed a stress-strain zoning model to categorize significant deformations, providing insights for reducing risks in rock-squeezing situations. Kamran et al. (2026) examined the potential for rock squeezing around tunnels by using a hybrid intelligent framework to enhance the performance of a classification algorithm. This proposed framework demonstrated a strong predictive capability of 96%, contributing to safer and more sustainable tunneling practices.

This paper investigates the squeezing condition using both experimental and numerical methods in Slope No. 2 of Parvadeh Mine No. 1. In this study, Slope No. 2 was chosen because the worst squeezing conditions occur at this site in the Parvadeh Mine. The aim is to assess the severity of squeezing and explore appropriate solutions to manage it, ensuring the safe continuation of excavation operations in the advancing tunnels while minimizing costs. Several empirical measures have been applied to address the issue of rock squeezing in the Parvadeh Mine. However, these measures were not based on scientific principles or standardized research, leading to challenges in effectively managing the severity of this phenomenon within the mine's tunnels. This study represents the first scientific attempt to tackle the problem of rock squeezing in the Tabas Parvadeh Mine. Currently, repair operations required for the maintenance of this tunnel are extremely high and difficult to control. Additionally, there have been several instances when work at the tunnel face had to be halted due to safety concerns. Work resumed only after addressing these safety issues and restoring the path to secure conditions.

II. SQUEEZING CONDITION IN THE PARVADEH 1 MINE

The Parvadeh coalfield is part of the larger Tabas coalfield, situated in the eastern region of central Iran, specifically to the west of South Khorasan Province. It is located on the northwestern edge of the Lut Desert, southwest of Tabas County. The area is bordered to the north by a completely flat desert plain and to the south by the Triassic-Jurassic highlands. To the east, it is bounded by the Camel Range, while the western boundary is defined by the heights of the Kalmard (Kamar Mahdi) region.

Parvadeh No. 1 coal mine, as the first mechanized coal mine in the country, has been designed for an annual production of 1.5–2.1 million tons of coal. Extraction in this mine is carried out using the mechanized long wall mining method. In the Parvadeh area, there are five coal layers. In mine-1, extraction operations are currently underway only in layer C1, which is approximately 2 meters thick and is thicker than the other coal layers. These operations are being conducted at significant depths using mechanized longwall method (TPCCO, 2024).

Several factors have contributed to the challenges in designing an appropriate and reliable support system for the tunnels excavated in the C1 coal seam. These factors include the sequence of sedimentary layers, the presence of faults, and high stresses due to proximity to the major Rostam fault. Additionally, the conditions at depths greater than 600 meters, the presence of groundwater, and the poor quality of the rock mass in both the hanging wall and footwall have made the task more difficult.

At present, the mine employs a combination of rock bolts and steel arches for tunnel support; however, this system has proven inadequate to withstand the applied stresses, resulting in significant tunnel convergence. In several locations, deformation has been so severe that damaged arches have had to be removed and bolts cut, necessitating continuous repair and rehabilitation of the development workings to ensure the continuation of mining operations.

In some sections, a coal layer is present at the tunnel floor. Owing to its relatively low strength, approximately 6 MPa, this layer is unable to effectively transfer loads from the roof to the floor, causing the support system to penetrate the coal. In water-bearing zones, this problem is further intensified, leading to substantial floor swelling. Moreover, the presence of a coal seam located close to the tunnel floor can similarly contribute to these effects and result in pronounced floor heave.

To address these challenges, steel arches with higher load-bearing capacity and reduced spacing are currently being implemented. Fig. 1 illustrates examples of severe squeezing conditions observed in the studied tunnel, accompanied by significant floor heave. In areas affected by convergence, resin and cement grouting are injected into the displaced strata to stabilize the opening and maintain operational space. After removing damaged supports, a new excavation profile is established and reinforced with an upgraded support system. In addition, convergence monitoring stations have been installed to systematically assess the performance of the supports.

III. ASSESSMENT OF SUPPORT REQUIREMENTS FOR SLOPE NO. 2 AT PARVADEH MINE USING HOEK'S METHOD (2006)

Hoek (1998) proposed the ratio of rock mass uniaxial compressive strength, σ_{cm}, to in situ stress, p_0, as an indicator of the likelihood of tunnel squeezing. Subsequently, Hoek and Marinos (2000) demonstrated that plotting tunnel strain, ε, against the ratio σ_{cm}/p_0 provides an effective means of evaluating tunneling performance under squeezing conditions. Based on this concept and an assessment of case histories from tunnels in Venezuela, Taiwan, and India, Hoek and Marinos (2000) developed the curve shown in Fig. 2 as a preliminary tool for estimating tunnel squeezing potential. Later, Hoek (2007), using axisymmetric finite element analyses covering a range of rock mass properties, in situ stresses, and support pressures *pi*, derived an approximate relationship for tunnel strain *ε*.

$$\varepsilon = \left(0.2 - 0.25\,\frac{p_i}{p_0}\right)\left(\frac{\sigma_{cm}}{p_0}\right)^{\left(2.4\frac{P_i}{p_0} - 2\right)} \qquad (1)$$

To better understand the trend of deformation behavior around the tunnel as described by Equation (1), Fig. 3 presents tunnel strain, ε, for a range of σ_{cm}/p_0 values and internal support pressures, p_i.

The study area consists of sedimentary layers, including coal, argillite, siltstone, mudstone, sandstone, and silty sandstone, which vary in thickness. For our calculations, we selected siltstone as it is representative of these layers. It is important to note that the presence of layering and water significantly impacts the rocks in this area, leading to a reduction in the quality of the rock mass. The data used for the calculations are detailed in Table 1.

Fig. 1. Examples of squeezing in Slope No. 2, Parvadeh 1 Mine: (a) movement of the roof causing deformation of the steel arches, (b) significant roof movement leading to severe deformation of the steel arches, (c) extreme roof movement resulting in almost complete closure of the tunnel, and (d) substantial heaving of the floor

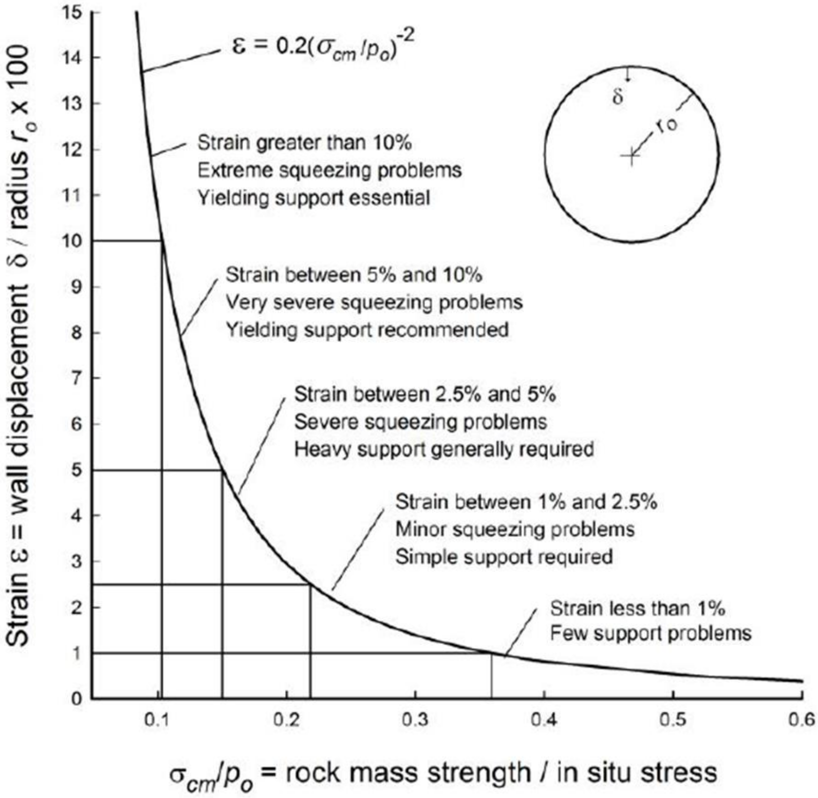

Fig. 2. Relationship between tunnel strain and ratio of rock mass strength to in situ stress (Hoek and Marinos, 2000)

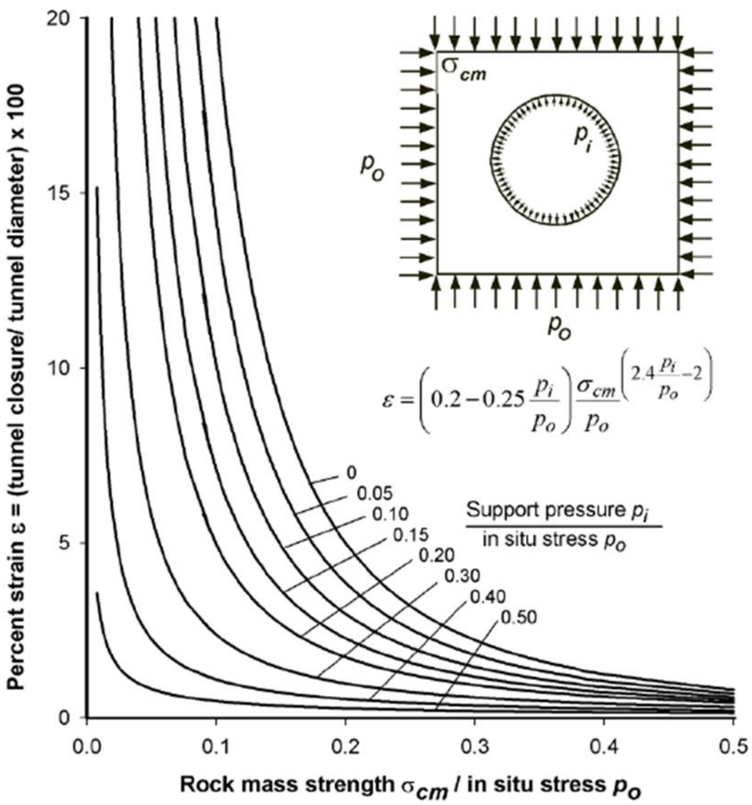

Fig. 3. Ratio of tunnel deformation to tunnel radius versus the ratio of rock mass strength to in situ stress for different support pressures (Hoek, 2007)

Table 1. Data utilized for calculations on slope No. 2 (TPCCO, 2024)

Parameter	unit	Value
UCS	MPa	32
C	MPa	1.1
ϕ	°	23.4
Compressive strength	MPa	1.81
Shear strength	MPa	0.035
E	GPa	7.4
Poisson' ratio		0.26
Depth	m	500
Density	kg/m3	2700

Based on the available data, the estimated compressive strength of the rock mass is 1.81 MPa. Additionally, considering the stratigraphy above Slope No. 2, as illustrated in Fig. 6, and the unit weight of the alternating layers listed in Table 2, the in situ stress (p_0) at a depth of 500 meters is estimated to be 13.5 MPa.

$$p_0 = \sigma_v = \sum \gamma \mathrm{h} = 13.5 \text{ MPa} \tag{2}$$

$$\frac{\sigma_{cm}}{p_0} = \frac{1.81}{13.5} = 0.134 \tag{3}$$

At this stage, we calculate the strain in the unsupported rock using (4) proposed by Hoek and Marinos (2000).

$$\varepsilon = 0.2\left(\frac{\sigma_{cm}}{p_0}\right)^{-2} = 11.25\% \tag{4}$$

Referring to Fig. 2, it is seen that the rock mass is in an area experiencing a strain greater than 10%, leading to very severe squeezing problems.

According to Hoek (2007), minor squeezing problems arise when tunnel strain is less than 2.5%. Therefore, this value can be regarded as the maximum allowable strain for a tunnel in squeezing ground conditions. Consequently, the support system should be designed to withstand a maximum strain of up to 2.5%.

Using the diagrams in Fig. 3, the required support pressure can be determined. By plotting an allowable tunnel strain of 2.5% on the vertical axis and a value of σ_{cm}/p_0 = 0.134 on the horizontal axis, an approximate ratio of p_i/p_0 = 0.3 is obtained. The corresponding value of p_i is then calculated as:

$$\frac{Pi}{P0} = 0.3 \rightarrow P_i = 0.3 \times 13.5 = 4.05\ MPa \tag{5}$$

The diagrams in Fig. 4 are then used to identify a support system capable of withstanding this pressure level. In these diagrams, the horizontal axis represents the tunnel width, which is 5.5 m for the tunnel under study, while the vertical axis denotes the maximum pressure acting on the support system, calculated as 4.05 MPa. As illustrated, the intersection of these two values lies on line 21, which can be identified from Fig. 4.

According to Fig. 4, a shotcrete lining with a thickness of approximately 300 mm is recommended for supporting the tunnel.

IV. FEM MODELING OF SLOPE NO. 2 OF PARVADEH MINE

Squeezing is defined as significant plastic deformation in soft rocks under pressure, without the initiation and propagation of macrocracks. This behavior is particularly well suited to finite element method (FEM) modeling. In this study, we examine the behavior of Slope No. 2 at a depth of 500 meters using RS2 software, a two-dimensional elasto-plastic finite element program designed for calculating stresses and displacements around underground openings.

Slope No. 2 is one of the four main tunnels in the mine network and must be maintained until the mine's closure. It serves as the primary route for transporting rail equipment, making it essential to preserve its original dimensions. To achieve this, a horseshoe cross-section shape has been chosen for the tunnel. The main support is provided through the use of rock bolts and yielding arches.

The dimensions of Slope No. 2 measure 5.5 meters wide at the bottom and 3.6 meters high at the center. The horizontal stress direction in the area relative to the tunnel's orientation is approximately 97 degrees. Fig. 5 displays the tunnel geometry created using the RS2 software.

The tunnel is surrounded by distinct geological layers, which should be represented as separate sections in the finite element model (see Fig. 6). The stratigraphy includes coal, siltstone, mudstone, argillite, sandy siltstone, and sandstone. The coal layer is positioned between two layers of siltstone. Above the siltstone layer in the hanging wall, there is a layer of sandstone. Notably, coal layer C2 is located approximately 6 meters above the main coal layer C1, which has a thickness of 1.85 meters.

Support type	Flange width - mm	Section depth - mm	Weight – kg/m	Curve number	Maximum support pressure p_{imax} (MPa) for a tunnel of diameter D (metres) and a set spacing of s (metres)
Wide flange rib	305	305	97	1	$p_{i\,max} = 19.9D^{-1.23}/s$
	203	203	67	2	$p_{i\,max} = 13.2D^{-1.3}/s$
	150	150	32	3	$p_{i\,max} = 7.0D^{-1.4}/s$
I section rib	203	254	82	4	$p_{i\,max} = 17.6D^{-1.29}/s$
	152	203	52	5	$p_{i\,max} = 11.1D^{-1.33}/s$
TH section rib	171	138	38	6	$p_{i\,max} = 15.5D^{-1.24}/s$
	124	108	21	7	$p_{i\,max} = 8.8D^{-1.27}/s$
3 bar lattice girder	220	190	19	8	$p_{i\,max} = 8.6D^{-1.03}/s$
	140	130	18		
4 bar lattice girder	220	280	29	9	$p_{i\,max} = 18.3D^{-1.02}/s$
	140	200	26		
Rockbolts or cables spaced on a grid of s x s metres	34 mm rockbolt			10	$p_{i\,max} = 0.354/s^2$
	25 mm rockbolt			11	$p_{i\,max} = 0.267/s^2$
	19 mm rockbolt			12	$p_{i\,max} = 0.184/s^2$
	17 mm rockbolt			13	$p_{i\,max} = 0.10/s^2$
	SS39 Split set			14	$p_{i\,max} = 0.05/s^2$
	EXX Swellex			15	$p_{i\,max} = 0.11/s^2$
	20mm rebar			16	$p_{i\,max} = 0.17/s^2$
	22mm fibreglass			17	$p_{i\,max} = 0.26/s^2$
	Plain cable			18	$p_{i\,max} = 0.15/s^2$
	Birdcage cable			19	$p_{i\,max} = 0.30/s^2$

Support type	Thickness - mm	Age - days	UCS - MPa	Curve number	Maximum support pressure p_{imax} (MPa) for a tunnel of diameter D (metres)
Concrete or shotcrete lining	1m	28	35	20	$p_{i\,max} = 57.8D^{-0.92}$
	300	28	35	21	$p_{i\,max} = 19.1D^{-0.92}$
	150	28	35	22	$p_{i\,max} = 10.6D^{-0.97}$
	100	28	35	23	$p_{i\,max} = 7.3D^{-0.98}$
	50	28	35	24	$p_{i\,max} = 3.8D^{-0.99}$
	50	3	11	25	$p_{i\,max} = 1.1D^{-0.97}$
	50	0.5	6	26	$p_{i\,max} = 0.6D^{-1.0}$

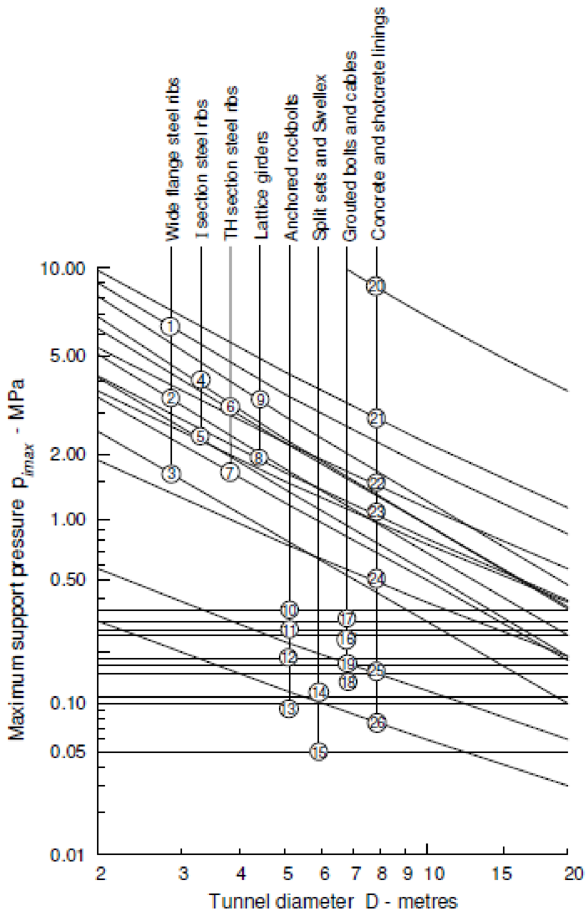

Fig. 4. Approximate maximum capacities for different support systems installed in circular tunnels. Note that steel sets and rock bolts are all spaced at 1 m (Hoek, 2007)

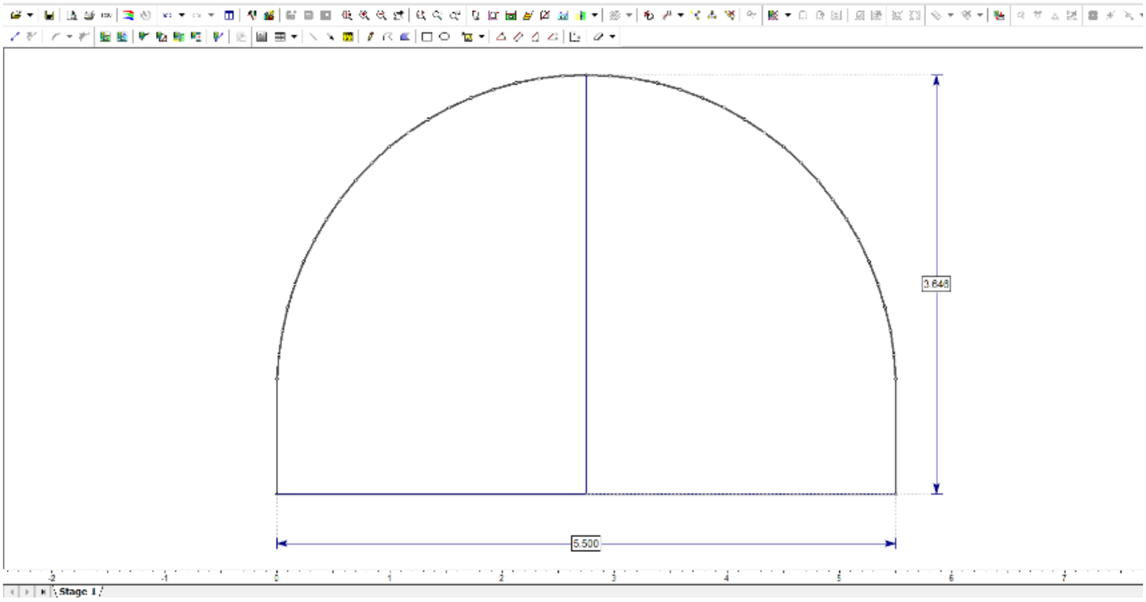

Fig. 5. Geometry of slope 2

Four-node elements were used to construct the FEM mesh. Fixed boundary conditions were applied in relation to the tunnel's depth being modeled. Fig. 7 shows a view of the constructed mesh created with RS2 software.

In this FEM model, the tunnel is located 300 meters above sea level. The piezometric groundwater level is at 800 meters, and the ground surface is at 900 meters, reflecting the actual conditions of the field.

V. GEOMECHANICAL PROPERTIES OF THE ROCKS SURROUNDING SLOPE NO. 2.

The coal-bearing formation consists of coal, with alternating layers of siltstone, mudstone, argillite, and sandstone. The main coal layer at the Parvadeh mine is the C1 layer, which has a thickness of approximately 1.85 meters. The geomechanical parameters for the rocks in Slope No. 2 are provided in Table 2.

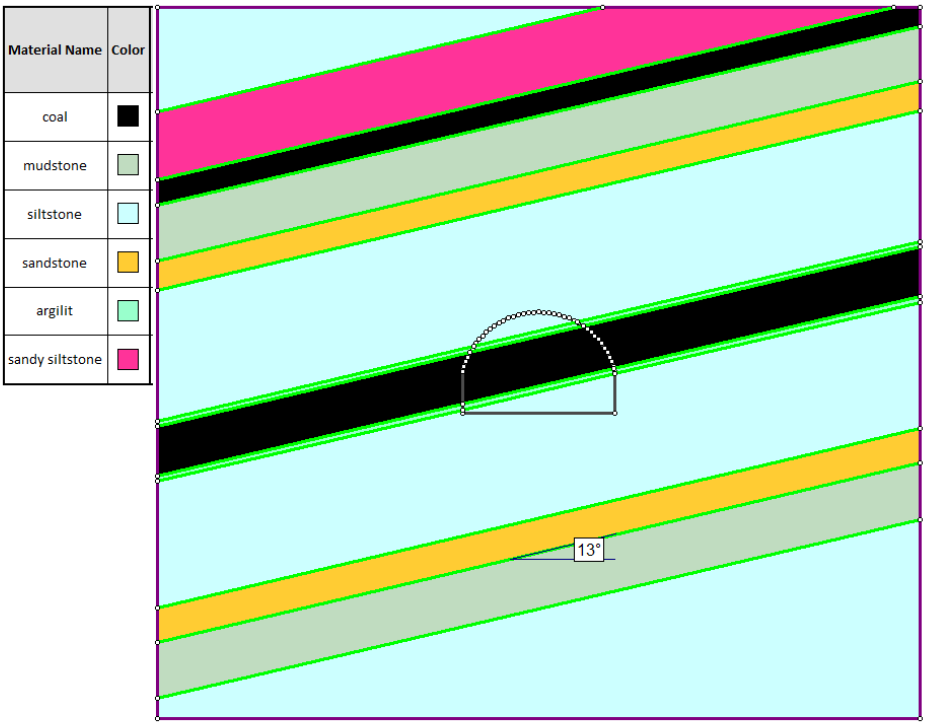

Fig. 6. Layering alternation around Slope No. 2

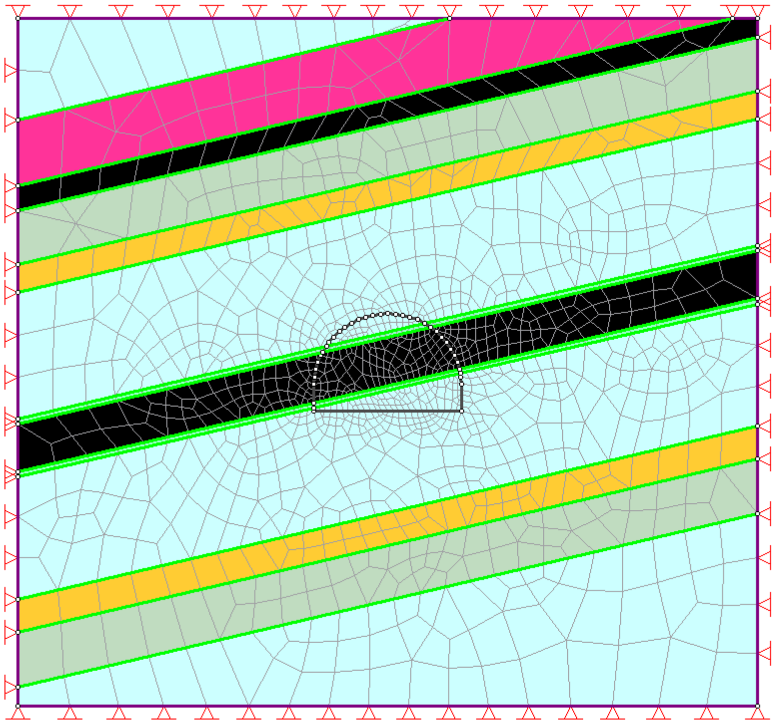

Fig. 7. The four-node mesh around Slope No.2

Table 2. The Geomechanical Parameters of Different Layers (TPCCO, 2024)

Property	Unit	argillite	mudstone	sandy siltstone	sandstone	siltstone	coal
Unit weight	MN/m^3	0.027	0.026	0.027	0.027	0.027	0.016
Young Modulus	*MPa*	2000	2838	2987	5281	2838	3160
Poisson' ratio	-	0.3	0.31	0.25	0.25	0.26	0.25
Internal friction	^{o}	35	18.62	31.75	21.69	24.12	34
Cohesion	*MPa*	10.5	0.94	0.44	8.69	1.3	0.33
Shear strength	*MPa*	0	0.013	2.6	6.3	2.5	0.002

VI. FEM MODELING OF SLOPE NO. 2 WITH AND WITHOUT A SUPPORT SYSTEM INSTALLATION

Once the numerical model of the tunnel is completed, the next steps will involve extracting the coal and creating the tunnel cross-section. Following this, a support system must be installed. In actual tunnel construction operations, rock bolts are typically installed immediately after drilling and are initially tensioned to 160 kN. Under these conditions, there is no opportunity for the discontinuities between the rock layers to open up. This creates a solid rock beam that counteracts the existing tension, which in turn affects the stability of the underground structure and allows sufficient time to install the main support system.

Rock bolts serve as active support components that enhance the shear strength of the roof rock. They accomplish this by increasing the adhesion between the layers or by countering the load applied by the roof rock. Rock bolts can connect multiple thin layers to form a thicker layer, thereby increasing the overall bearing capacity of the roof rock.

Through numerical modeling using the finite element method, the total displacement of the rock surrounding inclined Slope No. 2 was analyzed, as illustrated in Fig. 8. The displacement at the floor exceeds 9 meters, while at the walls and roof, it ranges between 5 and 6 meters.

To provide initial support for Slope No. 2, a total of 11 steel bolts, each 2.40 m in length, were installed in a fan-shaped pattern around the tunnel. The specifications of these bolts are summarized in Table 3. As illustrated in Fig. 9, the bolts are located within the yielding zone surrounding the tunnel and therefore have limited effectiveness in providing structural support or in reducing tunnel wall displacements (Fig. 10). Their primary function can be considered to be temporary roof stabilization in preparation for the installation of the main support system.

Given the level of displacement in the tunnel wall, it is clear that using rock bolts alone is insufficient to stabilize the wall. An additional system is necessary to address the pressures being exerted on the tunnel.

Table 3. Specifications of Metal Bolts Used in Slope No. 2 (TPCCO, 2024)

Parameter	Unit	Value
Length	*m*	2.4
Spacing	*m*	0.91
Diameter	*mm*	21.5
Ultimate tension load	*kN*	310
Ultimate shear	*kN*	254
Pretension load	*kN*	160

To determine the necessary support pressure for controlling tunnel convergence, various pressures were applied to the tunnel wall in the numerical model. This allowed us to measure the displacement values at eight specific points on the tunnel wall. The displacement values, recorded in meters at each point, can be found in Table 4 and Fig. 11.

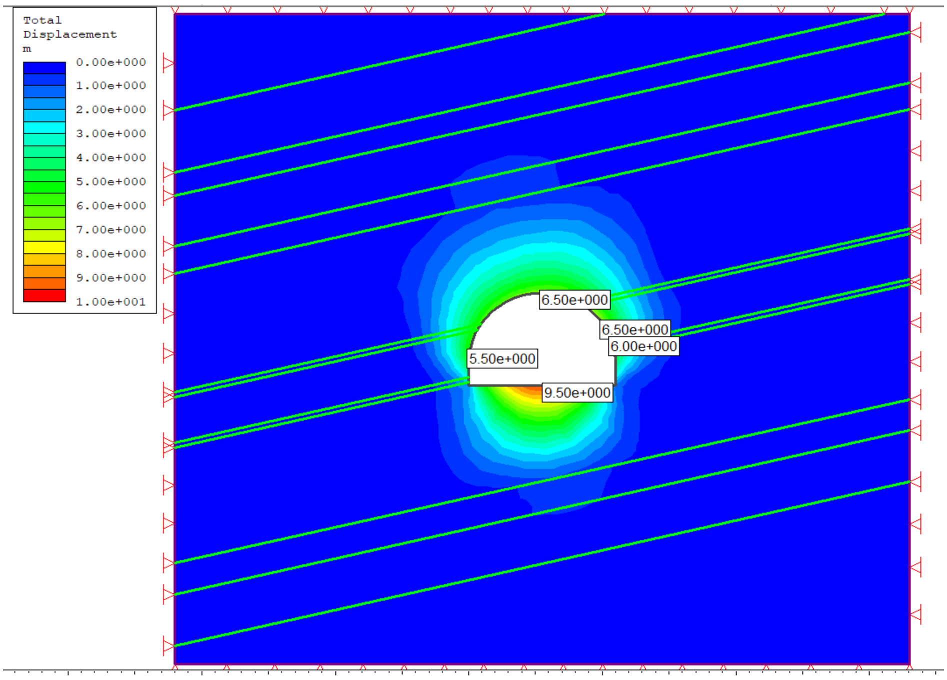

Fig. 8. Displacement of rock around the tunnel without the influence of the support system

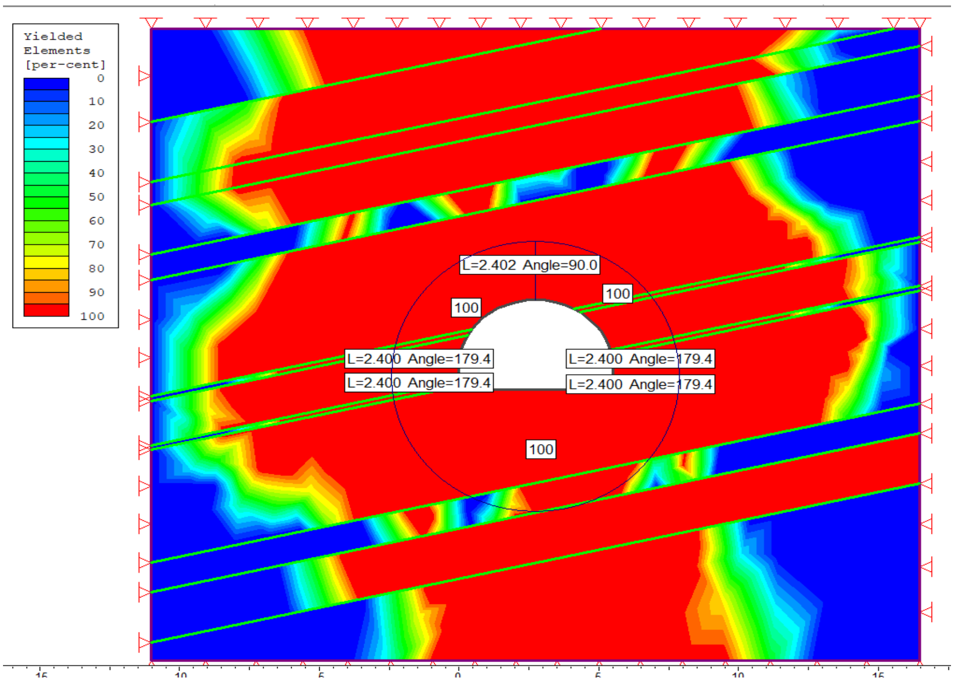

Fig. 9. Yielding area around the tunnel

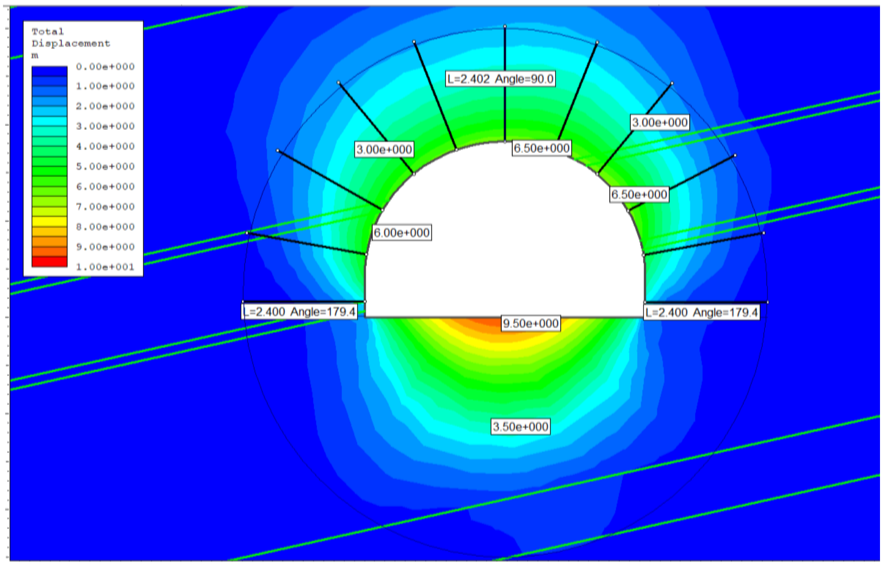

Fig. 10. Displacement of rock surrounding the tunnel as influenced by the support system

Table 4. Displacement Values Recorded at Eight Points on the Tunnel Wall Under Different Applied Pressures

No	Applied pressure, MPa	Disp. at point 1, m	Disp. at point 2, m	Disp. at point 3, m	Disp. at point 4, m	Disp. at point 5, m	Disp. at point 6, m	Disp. at point 7, m	Disp. at point 8, m
1	1	7.2	2.4	3.4	4.4	4.4	4	4	2.8
2	1.5	6	1.8	3.6	3.6	3.3	3	3.3	2.4
3	2	4.5	1.25	2.75	2.75	2.25	2	2.5	2
4	2.5	2.7	0.75	1.65	1.65	1.05	1.05	1.5	1.2
5	3	1.7	0.59	1.53	1.36	0.59	0.59	1.28	1.11
6	3.5	0.45	0.52	1.35	1.05	0.3	0.25	0.97	0.9
7	4	0.25	0.05	0.35	0.27	0.025	0.025	0.35	0.25
8	4.5	0.028	0.024	0.025	0.056	0.024	0.028	0.06	0.048
9	5	0.021	0.013	0.018	0.018	0.016	0.016	0.018	0.015

As shown in Table 4, as the load on the tunnel wall increases, convergence decreases. At a pressure of 4 MPa, the displacement at all studied points is less than 5 cm, which is below the allowable strain threshold of 2.5% proposed by Hoek. Additionally, the support pressure obtained from the numerical model is consistent with the value derived from Hoek's analytical method.

Fig. 11 shows the displacements of 8 different points of Slope 2 under different applied pressures. It should be noted that the applied pressures act in all directions, even on the tunnel floor.

VII. Selection of the Suitable Support System

Now that the rock pressure has been determined, a suitable support system must be selected to manage these pressures. As previously mentioned, when the rock mass is squeezing and of poor quality, passive support is essential due to the low effectiveness of rock bolts in these conditions. In such cases, flexible arches with circular sections are ideal as they allow for an even distribution of the load around the tunnel. However, since the Tabas Coal Parvadeh Company uses mechanized machines for tunnel excavation, a circular section cannot be implemented at the working face. Instead, TH-type arches with a horseshoe section are used for support.

Currently, TH36 arches spaced 0.6 meters apart, along with 11 bolts measuring 2.4 meters in length, support the tunnel. Table 5 provides the load-bearing capacities of TH-type arches with various sizes and support spacings. These values are estimated based on the formulas proposed by Hoek, as illustrated in Fig. 3. According to Table 5, the present support system exerts an equivalent pressure of 2.95 MPa on the tunnel walls, which is approximately 1 MPa lower than the 4 MPa support pressure identified in the previous section needed to mitigate tunnel convergence. Furthermore, Table 5 indicates that the maximum allowable spacing to withstand the applied pressure of 4 MPa corresponds to the TH40 type, which is spaced at 0.5 meters.

This type of arch is effective for stabilizing the roof and, to some extent, the walls. However, it may encounter issues under lateral pressures and additional stresses from the floor. If there is no support in the tunnel floor, swelling may occur, which can lead to significant problems in these conditions. Therefore, it is required to apply 30 cm shotcrete (or concrete slabs) to the tunnel floor as recommended by Hoek analytical method explained in section III.

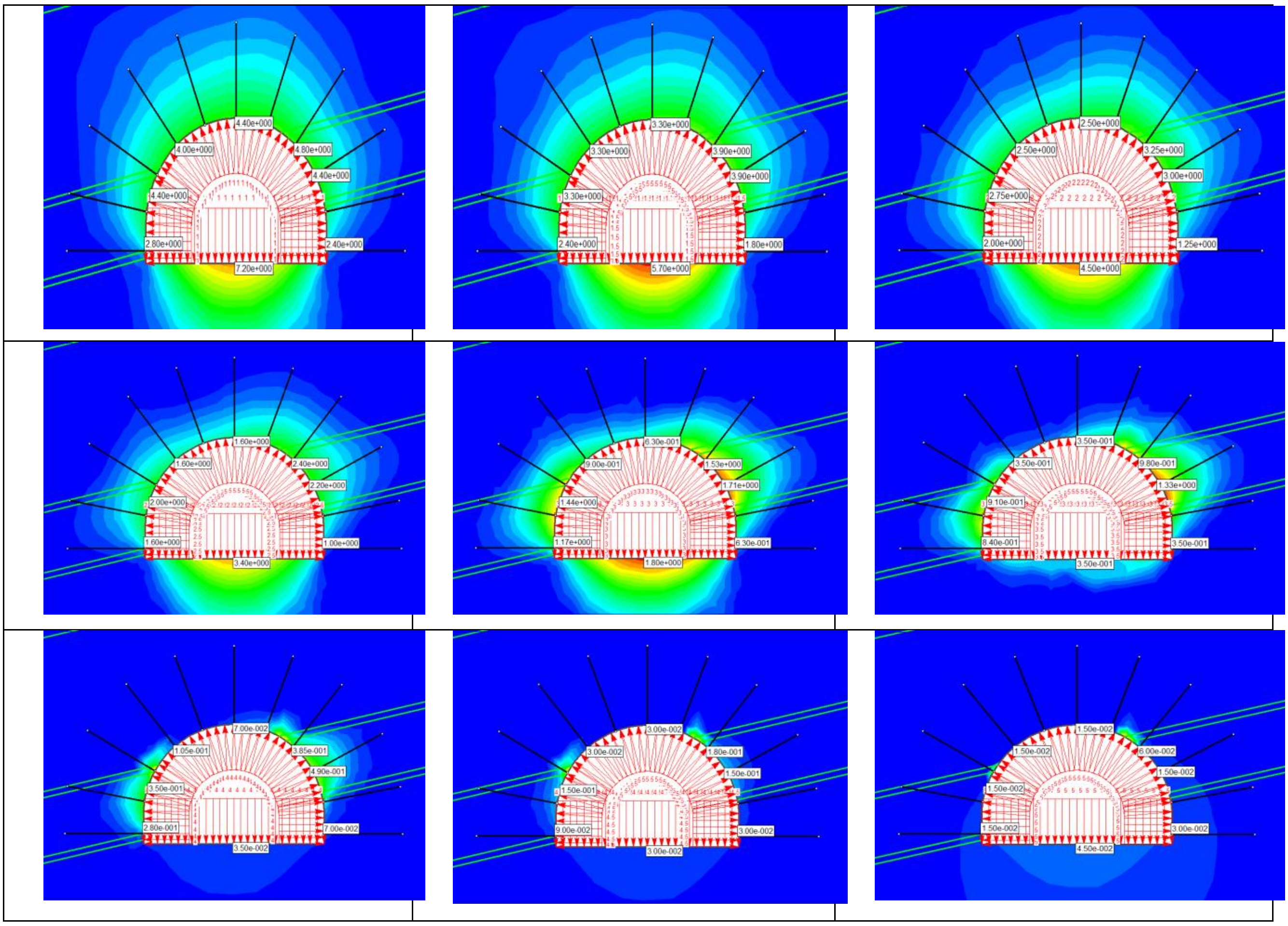

Fig. 11. Displacements of 8 different points on the Slope 2 walls under applied pressures ranging from 1-5 MPa

Table 5. Maximum Capacities of the Arches at Different Spacing

Spacing (m)	Bearing capacity (MPa)					
	TH21	TH29	TH36	TH38	TH40	TH44
1	1	1.4	1.8	1.9	2	2.2
0.8	1.3	1.8	2.2	2.3	2.5	2.8
0.6	1.7	2.4	3	3.1	3.3	3.7
0.5	2	2.8	3.5	3.7	4	4.4
0.4	2.5	3.5	4.4	4.7	5	5.5

VIII. CONCLUSION

Slope No. 2 is one of the four main tunnels of the Parvadeh No. 1 mine and must remain operational throughout the life of the mine. This tunnel also accommodates the installation of the main rail line and serves as the primary route for the transportation of personnel and equipment; therefore, maintaining its original cross-sectional dimensions is of critical importance. However, at depths exceeding 500 m, the poor quality of the rock mass, combined with the presence of groundwater, has made this task particularly challenging. Consequently, in many cases, severe convergence, deformation, and even structural failure have occurred following the installation of the existing support system.

Based on the results of the Hoek analytical method, which indicate support pressures exceeding 4 MPa as determined through empirical calculations, together with comparable results obtained from finite element modeling, it was concluded that TH36 steel arches installed at a spacing of 0.6 m are inadequate to resist the stresses acting on the excavated cross-section. Furthermore, under the current conditions and considering the extent of the yielded zone surrounding the tunnel, rock bolts with a length of 2.4 m were found to be ineffective as a primary support system and suitable only for temporary stabilization prior to the installation of the main support system.

Taking all results into account, the use of TH40 steel arches installed at a spacing of 0.5 m is considered capable of adequately withstanding the pressures exerted by the roof and sidewalls, provided that the tunnel floor is also reinforced using an additional support system, such as a 30cm shotcrete lining.

REFERENCES

Barton, N., Lien, R., Lunde, J. (1974). Engineering classification of rock masses for the design of tunnel support. Rock Mechanics and Rock Engineering, 6(4), 189-236.

Cheng, Y., Zhang, J., Wang, H. (2009). The influence of in-situ stress on rock deformation in underground coal mines. International Journal of Rock Mechanics and Mining Sciences, 46(7), 1205-1215.

Hoek E. (1998) Tunnel support in weak rock. Sedimentary Rock Engineering, ISRM Regional Symposium, Taipei, O. Chin-Der ed., pp. 281-292.

Hoek, E. & Marinos, P. (2000). Predicting tunnel squeezing problems in weak heterogeneous rock masses. Tunnels and Tunnelling International, 32(11), 45-51.

Hoek, E. (2001). Big tunnels in bad rock. Journal of Geotechnical and Geoenvironmental Engineering, 127(9), 726-740.

Hoek, E. (2007). Tunnels in weak rock, in Practical Rock Engineering (2007 ed.). E-book, www.rocscience.com.

Huang, Z., Liao, M., Zhang, H., Zhang, J., Ma, S., Zhu, Q. (2022). Predicting tunnel squeezing using the SVM-BP combination model. Geotechnical and Geological Engineering, 40, 1387–1405. https://doi.org/10.1007/s10706-021-01970-1.

Jaeger, J.C., Cook, N.G.W. (1979). Fundamentals of Rock Mechanics. 3rd ed. London: Chapman and Hall.

Kamran, M., Faizan, M., Wattimena, R.K., Armaghani, D.J., Asteris. P.G. (2026). A hybrid intelligent framework for the assessment and classification of squeezing potential of rocks around tunnels, Transportation Infrastructure Geotechnology. 13:56. https://doi.org/10.1007/s40515-026-00810-0.

Kang, H., Zhang, Y., Chen, Y. (2016). Analysis of rock squeezing behavior in deep coal mines: A case study from China. Journal of Mining Science, 52(3), 467-479.

Li, X., Liu, C., Wang, Y. (2015). Effects of water on the mechanical properties of coal rock under uniaxial compression. Coal Geology Exploration, 43(2), 15-20.

Luo, H., Wang, Z., Liu, K., Qiao, L., Qing, L. (2024) Stress-strain state zoning model and novel large deformation classification method for squeezing tunnels. Engineering Failure Analysis. 164, 108711.

Najm, S.J., Daraei, A. (2023). Forecasting and controlling two main failure mechanisms in the Middle East's longest highway tunnel. Engineering Failure Analysis. 146, 107091.

TPCCO (2024). Technical Office Report of Parvadeh No. 1 Mechanized Mine.

Wang, S., Xu, J., Zhang, Y. (2021). Real-time monitoring and prediction of rock mass deformation in underground coal mines using advanced technologies. Journal of Rock Mechanics and Geotechnical Engineering, 13(1), 123-135.

Yuan, H., Zhou, Z., Wu, X. (2020). Pre-mining geological investigation methods for assessing rock stability in coal mining areas. Mining Science, 27(2), 159-167.

Zhao, L., Zhang, X., Li, Z. (2019). Numerical modeling of squeezing behavior in deep coal mines: Implications for support design. Computers and Geotechnics, 113, 103-115.

Zhang, L., Chen, S., Liu, J. (2018). Economic analysis of support measures for managing squeezing conditions in underground coal mines. Resources Policy, 55, 1-9.